

The Role of Atmospheric Feedbacks in Abrupt Winter Arctic Sea Ice Loss in Future Warming Scenarios[✉]

CAMILLE HANKEL^a AND ELI TZIPERMAN^{a,b}

^a *Department of Earth and Planetary Sciences, Harvard University, Cambridge, Massachusetts*

^b *School of Engineering and Applied Sciences, Harvard University, Cambridge, Massachusetts*

(Manuscript received 15 July 2020, in final form 4 December 2020)

ABSTRACT: Winter Arctic sea ice loss has been simulated with varying degrees of abruptness across global climate models (GCMs) run in phase 5 of the Coupled Model Intercomparison Project (CMIP5) under the high-emissions extended RCP8.5 scenario. Previous studies have proposed various mechanisms to explain modeled abrupt winter sea ice loss, such as the existence of a wintertime convective cloud feedback or the role of the freezing point as a natural threshold, but none have sought to explain the variability of the abruptness of winter sea ice loss across GCMs. Here we propose a year-to-year local positive feedback cycle in which warm, open oceans at the start of winter allow for the moistening and warming of the lower atmosphere, which in turn increases the downward clear-sky longwave radiation at the surface and suppresses ocean freezing. This situation leads to delayed and diminished winter sea ice growth and allows for increased shortwave absorption from lowered surface albedo during springtime. Last, the ocean stores this additional heat throughout the summer and autumn seasons, setting up even warmer ocean conditions that lead to further sea ice reduction. We show that the strength of this feedback, as measured by the partial temperature contributions of the different surface heat fluxes, correlates strongly with the abruptness of winter sea ice loss across models. Thus, we suggest that this feedback mechanism may explain intermodel spread in the abruptness of winter sea ice loss. In models in which the feedback mechanism is strong, this may indicate the possibility of hysteresis and thus irreversibility of sea ice loss.

KEYWORDS: Arctic; Atmosphere–ocean interaction; Climate change; Feedback; Ice loss/growth; Model

1. Introduction

Arctic sea ice loss is both an early response to and a potential amplifier of global climate change, and as such, understanding its causes, mechanisms, and predictability is of great importance. Both the timing and magnitude of sea ice loss have implications for local communities and Arctic ecosystems. These concerns have motivated a significant body of research on Arctic sea ice loss. Much of this work has been focused on understanding present-day observations of Arctic sea ice, or on the predicted behavior of summer Arctic sea ice in near-future global warming scenarios. The focus of this work, however, is long-term projections of *winter* Arctic sea ice. Specifically, we are interested in exploring mechanisms that may lead to an abrupt disappearance of winter sea ice.

There has been much speculation about whether abrupt sea ice loss—both in summer and winter—can occur, and if such loss is potentially irreversible, indicating a hysteresis and bistability of the system (Ridley et al. 2012; Winton 2006). The debate on whether the loss of summer sea ice is expected to happen gradually or abruptly (Holland et al. 2006; Eisenman 2007, 2012; Wagner and Eisenman 2015; Ridley et al. 2012; Notz 2009) generally suggests that a gradual transition is more

likely. Results from toy models suggest that the transition to an ice-free Arctic summer could happen discontinuously on account of the ice-albedo feedback. However, results from including additional feedbacks in simple models (Eisenman and Wettlaufer 2009; Eisenman 2012) and from more realistic models that include latitudinal and seasonal variations as well as fully coupled global climate models (GCMs) all indicate that this transition will happen gradually (Wagner and Eisenman 2015; Notz 2009; Armour et al. 2011).

Abrupt sea ice loss in winter is a more robust feature than abrupt summer sea ice loss for both toy models (Abbot et al. 2011; Abbot and Tziperman 2008b) and GCMs (Hezel et al. 2014; Drijfhout et al. 2015; Bathiany et al. 2016), and there are several mechanisms that have been suggested regarding its drivers and reversibility. Abbot and Tziperman (2008b) and Abbot et al. (2011) used a column model to show that abrupt sea ice loss in winter can result from a convective cloud feedback represented by a saddle node bifurcation. Armour et al. (2011) present an alternate view by showing that winter sea ice loss is reversible in one GCM (CCSM3), and thus not part of a bifurcation and hysteresis in that model. Other work still (D.-S. R. Park et al. 2015; H.-S. Park et al. 2015; Leibowicz et al. 2012; Gong et al. 2017) has focused on the historical and present-day loss of winter sea ice, which of course has not yet displayed any threshold behavior, but is shown to be greatly affected by winter longwave radiation, which we examine closely in this study.

Overall, we identify a need for further understanding of the effect of positive feedbacks on long-term winter sea ice loss and its implications for sea ice predictability in a future Arctic. Analysis of GCMs run under the extended RCP8.5 scenario in

[✉] Supplemental information related to this paper is available at the Journals Online website: <https://doi.org/10.1175/JCLI-D-20-0558.s1>.

Corresponding author: Camille Hankel, camille_hankel@g.harvard.edu

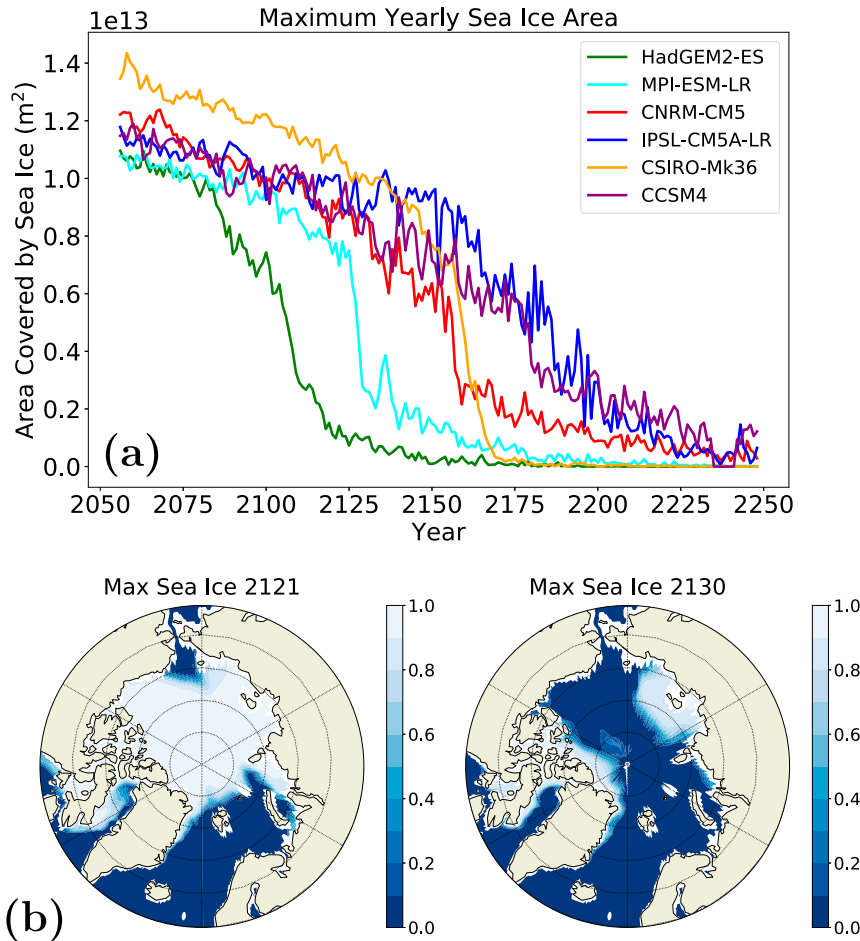


FIG. 1. (a) Yearly maximum sea ice area evolution in the extended RCP8.5 scenario for the six models considered in this study. Models CSIRO Mk3.6, HadGEM2-ES, and MPI-ESM-LR all exhibit a period of accelerated winter sea ice loss, potentially indicative of a threshold or “tipping point” behavior. (b) Example of the abrupt winter sea ice loss for one of the models, MPI-ESM-LR. Shown is the yearly maximum sea ice fraction before and after the abrupt change, only 9 years apart.

phase 5 of the Coupled Model Intercomparison Project (CMIP5; Taylor et al. 2012) shows winter sea ice to disappear at different speeds in different models (Hezel et al. 2014; Drijfhout et al. 2015). Figure 1a shows the time series of yearly maximum sea ice area for six such models, with some models notably revealing an apparent abrupt melting (“tipping point”-like behavior) in winter Arctic sea ice even when summer sea ice melting occurs gradually. Figure 1b demonstrates how abrupt this winter sea ice loss is for one model, MPI-ESM-LR. As mentioned above, this apparent tipping point could be indicative of the occurrence of a bifurcation due to the crossing of a CO_2 forcing threshold. If so, one may expect hysteresis, in which complete winter sea ice loss is irreversible beyond a certain forcing value, which would have profound implications for the climate system as a whole.

Such a bifurcation and hysteresis of winter sea ice were proposed to be a possible result of a “convective cloud feedback” mechanism in the context of both future (Abbot and Tziperman 2008b) and past (Abbot and Tziperman 2008a)

warm climates, and this feedback was studied using analytic models (Abbot and Tziperman 2009), GCMs (Abbot et al. 2009), and a superparameterized coupled GCM (Arnold et al. 2014). The convective cloud feedback relies on the onset of wintertime convection over open ocean to drive convection and deep convective clouds, the longwave (LW) radiative effect of which suppresses sea ice growth. Interestingly, we find here that downward LW radiation plays a significant role in affecting the abruptness of winter sea ice loss, but that while wintertime Arctic atmospheric convection indeed occurs in all models examined at high enough CO_2 , the LW cloud radiative effect does not seem to be a major player.

Bathiany et al. (2016) looked closely at the apparent wintertime sea ice tipping point in one of the GCMs analyzed here (MPI-ESM) and found that the tipping point persists even when the ice-albedo feedback and the convective cloud feedback are disabled; subsequently, they suggested that the freezing point provides a natural threshold that could explain

the abrupt sea ice loss without any positive feedbacks. While the threshold behavior of the freezing point is certainly important, it alone without the inclusion of positive feedbacks cannot explain the variability in the abruptness of sea ice loss across models, nor the seemingly homogenous and monotonic nature of the sea ice loss in some models.

Thus, the goal of this work is to examine the role of positive feedbacks in affecting the abruptness of winter Arctic sea ice melting across GCMs run in CMIP5. Noting the extensive literature that outlines the importance of air–sea exchanges for feedback mechanisms in the Arctic (Taylor et al. 2018; Smith et al. 2017), we focus on *local* coupled sea ice–ocean–atmospheric mechanisms. Previous work (Burt et al. 2016; Krikken and Hazeleger 2015) suggested that both ocean and atmospheric heat transport contribute minimally to the heat budget of the Arctic, and more importantly tend to decrease over the course of global warming GCM simulations. While we do not rule out the potential contribution of remote feedbacks driven by ocean or atmospheric heat transport, we do not analyze these here.

Other studies have examined and quantified the role of positive feedbacks in driving Arctic amplification (Taylor et al. 2013; Bintanja et al. 2011; Pithan and Mauritsen 2014; Block and Mauritsen 2013; Goosse et al. 2018; Boeke and Taylor 2018; Feldl et al. 2020; Stuecker et al. 2018) but none have addressed the relationship between these positive feedbacks and abrupt wintertime sea ice loss. Bintanja et al. (2011) and Pithan and Mauritsen (2014) showed that a positive lapse-rate feedback is active in the Arctic due to the reduced efficiency of thermal emission that accompanies the strong surface temperature inversion, and that this feedback is one of the main contributors to Arctic amplification. Feldl et al. (2020) extended this work to show that a strong lapse-rate feedback is correlated to a strong surface albedo feedback, suggesting that increased upward turbulent heat fluxes due to reduced ice coverage supply the heat that drives surface-amplified warming, and thus the two aforementioned feedbacks should be considered in conjunction. Stuecker et al. (2018) suggested that local rather than remote feedbacks drive the amplified warming in the Arctic in coupled models, by applying regional CO₂ forcings, and again found that the positive lapse-rate feedback appears to be the most important local feedback.

We propose that what Burt et al. (2016) referred to as a wintertime “ice-insulation feedback” together with a springtime ice-albedo feedback, linked together by seasonal heat storage by the ocean, contribute significantly to the simulated abrupt winter sea ice loss. Boeke and Taylor (2018) sought to explain the variability in Arctic amplification simulated by GCMs with a similar positive feedback mechanism, while here we seek to explain the variability in the abruptness of winter sea ice loss across models. Specifically, we use a quantitative feedback analysis to show that models with a weaker feedback mechanism have less abrupt winter sea ice loss, while models with a stronger feedback show more abrupt sea ice loss, which qualitatively resembles a tipping-point behavior. Several methods for quantifying feedbacks have been proposed by previous work, including the radiative kernel technique (Soden et al. 2008; Block and Mauritsen 2013; Pithan and Mauritsen

2014; Goosse et al. 2018), partial temperature contributions (Boeke and Taylor 2018), and the Climate Feedback Response Analysis Method (CFRAM; Lu and Cai 2009a). For reasons discussed below, we find the radiative kernel technique and the CFRAM to be less suitable for the abrupt winter sea ice loss problem. Instead, we use the partial temperature contributions (PTCs) approach of Boeke and Taylor (2018).

The positive feedback we find to play a role in affecting the abruptness of winter sea ice loss is as follows. In a seasonally (summer) ice-free future Arctic, the warm, open ocean needs to cool in autumn and winter before winter sea ice can begin to regrow. As the atmosphere cools in winter faster than the ocean, strong vertical temperature and moisture gradients are established that lead to increases in upward latent and sensible heat fluxes (Screen and Simmonds 2010). These turbulent fluxes warm and moisten the lower atmosphere, which in turn causes the atmosphere to trap and re-emit longwave radiation back to the surface. The increase in downwelling longwave at the surface further suppresses ocean cooling, and delays sea ice freeze-up, which allows the turbulent heat fluxes to persist later into winter. The delayed freeze-up causes the maximum sea ice concentration achieved in March or April to be lower yet, which in turn leads to increased springtime shortwave absorption due to the lower albedo. This extra heating by shortwave (SW) radiation not only melts the seasonal sea ice more quickly, but also warms the summer ocean. Some of this heat is stored in the upper ocean, which sets up conditions for an even warmer open ocean at the start of the ice-growing winter season. This completes one full feedback cycle, and subsequently leads to even stronger winter latent and sensible heat fluxes, thus to a warmer and moister atmosphere, more downwelling longwave, and even more delayed sea ice freeze-up and lower maximum sea ice area.

In section 2 we describe the model output used, the partial temperature contribution method (Boeke and Taylor 2018), and the measure used for quantifying the abruptness of winter sea ice loss. Next in section 3 we discuss the results of the analysis of feedback strength in different seasons and its connection to the abruptness of wintertime sea ice loss, and we conclude in section 4.

2. Methods

We use results from six global climate models (GCMs) run under the extended RCP8.5 scenario in CMIP5 (Taylor et al. 2012). Of the models that took part in CMIP5, only nine were run for the extended RCP scenarios (which run through 2300), and each model only has one ensemble member for the RCP8.5 scenario. We perform our analysis of abrupt sea ice loss on six of these nine models. Of the models that were excluded, two never fully lost their winter sea ice by the end of the simulation (GISS-E2-H and GISS-E2-R), and one did not have data available for download at the time of this study (BCC_CSM1.1).

We hypothesize that the varying strength of the proposed feedback across different models produces a range in the abruptness of simulated winter sea ice area loss. Indeed, we see from Fig. 1a that even within the models that qualitatively appear to have a tipping point, some still experience more

abrupt winter sea ice loss than others—for example, compare CSIRO Mk3.6 with HadGEM2-ES. Thus, there is a need for both a quantitative metric of the abruptness of sea ice loss and a quantification of the strength of the proposed feedback.

To quantify the strength of the proposed feedback, we calculate the PTCs of different mechanisms that play a role in the year-to-year feedback cycle (such as increases in downwelling longwave radiation or changes in surface albedo) by decomposing the surface energy budget, following [Boeke and Taylor \(2018\)](#). This analysis can be easily done with standard CMIP5 output data and allows for comparison with [Boeke and Taylor \(2018\)](#), who propose a similar year-to-year feedback cycle for explaining Arctic amplification in the twenty-first century alone. Although this method calculates feedback strength based on contributions to surface temperature warming and not to sea ice loss specifically, Arctic surface temperatures and sea ice area are generally tightly coupled ([Feldl et al. 2020](#)) and thus we expect the feedback mechanisms analyzed here to play a role in driving changes in both.

Directly following [Boeke and Taylor \(2018\)](#), the surface energy budget can be decomposed as

$$Q = (1 - \alpha)S_{\text{dn}} + F_{\text{dn}} - \epsilon\sigma T_s^4 - (S + L), \quad (1)$$

where Q represents the storage and transport of heat by the ocean, α is the surface albedo calculated as the upwelling shortwave clear-sky radiation divided by the downwelling shortwave clear-sky radiation at the surface, S_{dn} is the all-sky downwelling shortwave radiation, F_{dn} is the all-sky downwelling longwave radiation, $\epsilon\sigma T_s^4$ is the upwelling longwave radiation (where ϵ is the emissivity of the surface, taken to be 1, and T_s is the surface temperature), S is the upward sensible heat flux, and L is the upward latent heat flux. Equation (1) is taken to be satisfied at all grid points and at all times, and Q is thus computed as a residual of the other variables. Considering the change in Eq. (1) between two different times in the simulation, solving for T_s , and linearizing ΔT_s^4 yields

$$4\sigma T_s^3 \Delta T_s = \Delta[(1 - \alpha)S_{\text{dn}}] + \Delta F_{\text{dn}} - \Delta Q - \Delta S - \Delta L. \quad (2)$$

In this study, the Δ values represent changes in the given variables between the beginning and end of each model's period of abrupt winter sea ice loss, the identification of which is described below. Last, by considering the cloud radiative effect following [Lu and Cai \(2009b\)](#) to be $\Delta\text{CRE} = (1 - \bar{\alpha})\Delta S_{\text{dn,clr}} + \Delta F_{\text{dn,clr}}$ such that the effects of changing albedo are separated from radiative effects of changing clouds, substituting into Eq. (2) yields the final form of the PTC approach used here:

$$\Delta T_s = \frac{-(\Delta\alpha)(\overline{S_{\text{dn}}} + \Delta S_{\text{dn}}) + \Delta\text{CRE} + (1 - \bar{\alpha})\Delta S_{\text{dn,clr}} + \Delta F_{\text{dn,clr}} - \Delta Q - \Delta S - \Delta L}{4\sigma T_s^4}, \quad (3)$$

where $\bar{\alpha}$ and $\overline{S_{\text{dn}}}$ represent mean-state values, calculated as a 20-yr average centered around the starting year of the period of abrupt sea ice loss. The terms on the right-hand side represent contributions from the surface albedo feedback (SAF), cloud radiative effect (CRE), changes in clear-sky shortwave radiation, changes in clear-sky longwave radiation, changes in ocean heat storage and transport, changes in sensible heat flux, and changes in latent heat flux. The strength of these feedback mechanisms during the period of abrupt winter sea ice loss specifically measures their influence on the surface warming, which, as explained above, we assume quantifies their contribution to sea ice loss as well.

In this study we do not use the radiative kernel technique for quantifying radiative feedbacks that was outlined by [Soden et al. \(2008\)](#) and applied in subsequent studies (see [section 1](#)). Because the radiative feedback method assumes a small linear perturbation to the climate state for which the kernel is derived, we expect it to introduce large errors when being applied to a period of rapid and large change such as the period of abrupt winter sea ice loss. Indeed, [Block and Mauritsen \(2013\)](#) show that the MPI-ESM-LR radiative kernel is strongly state dependent, with the surface albedo feedback kernel being reduced by half when considered in a $4 \times \text{CO}_2$ state versus a control state. Thus, even using a radiative kernel derived from climate state immediately prior to the abrupt winter sea ice loss is likely to be insufficient for representing the response of TOA radiation to feedback variables throughout the entire period of abrupt sea ice loss. Similarly, [CFRAM \(Lu and Cai 2009a\)](#)

assumes a small perturbation to atmospheric energy fluxes and requires output variables that are not consistently available in the CMIP5 archive (such as vertical profiles of horizontal and vertical energy transports). The more generalized feedback quantification framework proposed by [Goosse et al. \(2018\)](#) [their Eq. (1)] is useful for comparing radiative and non-radiative feedbacks (which is not our primary concern here) and also requires output from simulations with specific feedback mechanisms turned off, to which we do not have access.

We identify the years of abrupt winter sea ice loss by fitting a sigmoid function to the time series of maximum yearly sea ice area of the form $f(x) = -L/\{1 + \exp[-k(x - x_0)]\} + b$. We then choose the start and end of the period of abrupt sea ice loss for each model to be $x_0 \pm 1.5/k$ (Fig. S1 in the online supplemental material). These years are used as the period of change that is considered in the calculation of PTCs, where Δ values are calculated as the difference between the 20-yr averages centered around the start and end years.

Thus, we consider the PTCs of the different surface processes during the year range corresponding to an abrupt winter sea ice loss. Because the length of the period of abrupt winter sea ice loss is different across models, we divide the PTCs by this time length so that their units are kelvins per year, allowing us to compare PTCs across models. We limit the regional scope of this calculation to the areas of the ocean that had at least 10% maximum yearly sea ice concentration at the start of the period corresponding to the abrupt winter sea ice loss. We do so because an alternative strategy such as including the entire

Arctic area above a certain latitude would include changes in variables over parts of the ocean that were ice free throughout the entire simulation. Thus, PTCs are calculated at all grid points that satisfy this criterion, and then averaged according to grid cell area to give a single PTC for each mechanism for the region of sea ice loss as a whole. We tested cutoff values other than 10% for the maximum yearly sea ice cover and found that our results are insensitive to the value used. We note here that studies attempting to calculate the sensitivity of a certain climate variable to sea ice change might calculate the change in that variable normalized by a unit change in sea ice. However, this normalized ratio would not distinguish between two models that lost the same amount of sea ice and had the same change in a given feedback variable, but over different periods time, not allowing us to distinguish models with abrupt versus gradual sea ice loss. This is why we focus the bulk of our analysis (e.g., Figs. 2 and 3) on PTCs in terms of their contribution per year, which captures the abruptness of changes in surface heat fluxes (see Fig. S2 in the online supplemental material for an analysis using a different normalization of the PTC analysis).

To quantify the level of abruptness of winter sea ice loss across models, we perform a linear regression on the time series of sea ice area within the calculated year ranges described above and use the slope of the regression line (with units of meters squared per year) as the metric for ranking the abruptness of winter sea ice loss for all models. We then compare the strength of the local mechanisms that make up the year-to-year feedback cycle using PTCs with the abruptness of winter sea ice loss across models to directly test our hypothesis that the range in strength of local feedbacks can explain the range in abruptness of winter sea ice loss.

Certainly, other metrics for quantifying the level of abrupt sea ice loss could be used, and we address some of those possibilities here. First, one could consider defining a metric based on sea ice volume rather than area, and in fact we find that ice volume also shows abrupt changes in the models that show it for ice area (not shown). While this would capture more information about sea ice thinning, sea ice area may be more relevant for atmosphere–ocean coupling, which is our primary interest here. Differences in sea ice thinning rates across models may affect the surface albedo feedback among other factors but are not fully explored in this study. In addition, one could use the magnitude of sea ice area that is lost in a particularly abrupt phase instead of the rate of loss. We find that using this metric does not affect our main results (not shown).

3. Results

We now examine air–sea heat fluxes that play a role in the proposed year-to-year feedback cycle during the disappearance of winter sea ice area by analyzing their PTCs (kelvins per year, reflecting the contribution of each process to the rate of change of surface temperature during the period abrupt sea ice loss; see section 2). If the proposed year-to-year feedback cycle is strong, we expect PTCs associated with key air–sea exchanges to be large. For example, because we hypothesize that warmer ocean temperatures at the end of autumn lead to

increased heat and moisture fluxes to the atmosphere, we expect strong negative latent heat flux (LHFX) and sensible heat flux (SHFX) PTCs, particularly in autumn and in winter. These increased turbulent heat fluxes lead to increased downwelling longwave from the atmosphere, which we expect to be reflected in either the longwave clear-sky (LWCS) or cloud radiative effect (CRE) PTCs. In the springtime, when shortwave radiation increases, we expect that a lower sea ice area maximum in spring leads to increased shortwave absorption by the ocean, which suppresses sea ice growth the following year. This would be reflected in a large surface albedo feedback (SAF) PTC. Overall, we expect that models with a stronger net positive year-to-year feedback cycle will show larger yearly PTCs and similarly will show more abrupt sea ice loss, and thus we start our analysis by comparing these two quantitative metrics. We then look further into the drivers of one of the most critical PTCs: LWCS. Last, we examine the critical role of the ocean in providing a memory, *locally* storing the extra heat absorbed from the springtime reduced albedo, and later fueling the air–sea temperature difference needed for the turbulent heat fluxes that drive the wintertime warming and suppression of sea ice regrowth.

We start by comparing the magnitude of all of the PTCs with the abruptness of winter sea ice loss for all models, recognizing that there could be a continuous range in both feedback strength and winter sea ice loss abruptness. Figures 2a–f and 2h show the yearly PTC for each mechanism represented in Eq. (3) plotted against the abruptness metric for winter sea ice loss (see section 2) for each model. A linear regression is fitted to each scatterplot, and the legend shows the R^2 value of this regression. For six models and therefore 4 degrees of freedom, R^2 is significant at the 95% level for $R^2 > 0.658$ following a two-tailed t test. The statistically significant correlations in Figs. 2a and 2b demonstrate that the PTCs of the surface albedo feedback and changes to longwave clear-sky radiation respectively contribute more warming per year for models with more abrupt winter sea ice loss. Similarly, Figs. 2e and 2f show that models with more abrupt winter sea ice loss have larger negative LHFX and SHFX PTCs, respectively. Interestingly, Fig. 2c shows that the shortwave clear-sky (SWCS) PTC is more negative for models with more abrupt sea ice loss, possibly due to increased shortwave absorption by water vapor in models that lose sea ice more rapidly. Yearly PTCs of the cloud radiative effect and ocean heat storage Q are not strongly correlated with the abruptness of winter sea ice loss, as shown in Figs. 2d and 2h respectively.

The strong correlations in Figs. 2a, 2b, 2e, and 2f are consistent with the hypothesized year-to-year feedback cycle. Notably, the surface albedo feedback and LWCS PTCs have the largest magnitudes of all the PTCs, contributing on the order of $\sim 0.1 \text{ K yr}^{-1}$ each, which indicates that they are the most important components of the year-to-year feedback cycle. The large magnitude of the LWCS PTC is consistent with past studies (Burt et al. 2016; D.-S. R. Park et al. 2015; H.-S. Park et al. 2015; Abbot et al. 2009) that show longwave radiation to be a critical variable for suppressing sea ice growth. When the yearly PTCs are broken down by season (not shown), we see that the yearly LWCS PTC is largely driven by

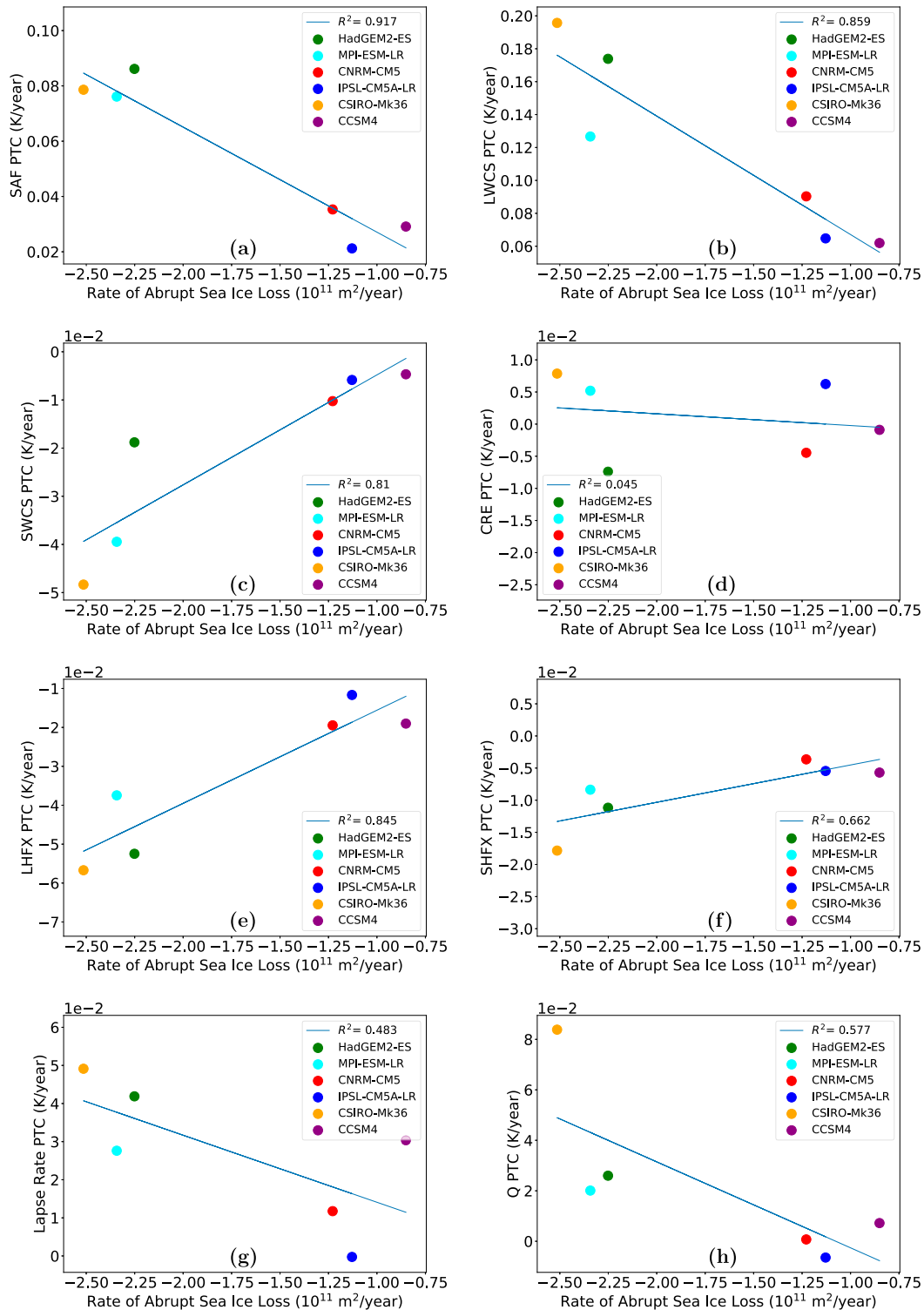


FIG. 2. Quantifying the strength of the different mechanisms that make up the year-to-year feedback cycle using PTCs. All panels depict the yearly PTC, which is the PTC over the period of abrupt winter sea ice loss divided by the number of years in the abrupt period. The PTCs depicted are from changes in (a) surface albedo feedback, (b) longwave clear-sky radiation, (c) shortwave clear-sky radiation, (d) cloud radiative effect, (e) upward latent heat flux, (f) upward sensible heat flux, (g) lapse rate, and (h) ocean heat storage and transport.

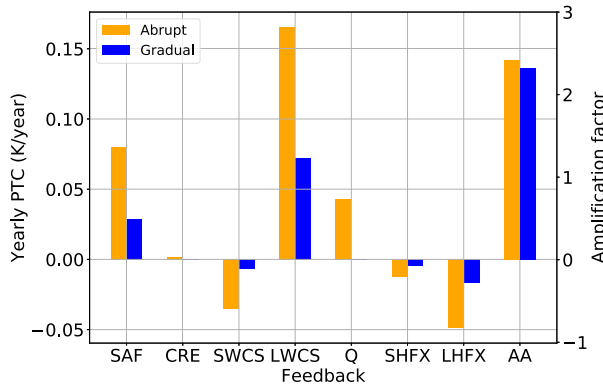


FIG. 3. Yearly PTCs as averages for two groups of models: those with a qualitatively apparent period of abrupt winter sea ice loss (MPI-ESM-LR, CSIRO Mk3.6, and HadGEM2-ES), and those with qualitatively gradual winter sea ice loss (IPSL-CM5A-LR, CNRM-CM5, and CCSM4). The rightmost bars and corresponding right y axis show the level of Arctic amplification (AA) for the two groups of models between the start of the simulation and the end of the simulation, calculated as the mean temperature change poleward of 60°N, divided by the global mean temperature change.

changes in the autumn [September–November (SON)] and winter [December–February (DJF)], whereas large SAF PTC is driven by changes in spring [March–May (MAM)] and, to a lesser degree, summer [June–August (JJA)]. Similarly, the LHFx and SHFX PTCs are largely driven by changes in winter, consistent with the year-to-year feedback cycle. The larger *negative* PTC seen for LHFx and SHFX (Figs. 2e,f) for models with more abrupt sea ice loss may seem nonintuitive since these processes represent surface cooling. However, this is consistent with the faster summer surface warming in these models, which leads to the faster cooling response in autumn and winter reflected in Figs. 2e and 2f. The strong upward turbulent heat fluxes warm and moisten the lower atmosphere, increasing LWCS and therefore helping to drive the positive LWCS PTC seen especially for the models with more abrupt winter sea ice loss.

Figure 4c shows the rate of change of winter convective precipitation during the period of abrupt sea ice loss versus the abruptness metric. Here, convective precipitation is used as a proxy for strength of convection. Because neither the strength of convection nor the CRE PTC (Fig. 2d) shows strong correlations with the abruptness of sea ice loss, we conclude that a convective cloud feedback mechanism from past studies (Abbot and Tziperman 2008b; Abbot et al. 2009) is unlikely to play an important role in directly affecting the abruptness of change of surface temperature or sea ice loss. However, it is important to note that we find wintertime convection to be active in all models (except in IPSL-CM5A-LR, which did not show an abrupt loss), a surprising finding consistent with the convective cloud feedback mechanism (Abbot and Tziperman 2008b; Abbot et al. 2009). This suggests that convection could lift the extra moisture and heat supplied at the surface to heights in the atmosphere where it would contribute to the strong clear-sky radiative effect that we see.

Changes in LWCS at the surface can be attributed to changes in atmospheric temperature (both due to uniform warming and changes in the lapse rate), as well as to changes in atmospheric humidity that increase emissivity. In Figs. 4a and 4b, we show the rate of change of winter atmospheric specific humidity and temperature, respectively, at 850 hPa during the years of abrupt sea ice loss, plotted against the abruptness of winter sea ice loss for each model. We focus on the winter average (DJF) temperature and moisture since, as noted above, the winter component of the LWCS PTC is largely responsible for the large annual LWCS PTC. The statistically significant correlations ($R^2 > 0.658$) in both panels indicate that both winter humidity and air temperature are increasing faster in models with more abrupt sea ice loss, and thus both could be responsible for the winter increases in LWCS.

To further differentiate between the contributions of temperature and moisture changes to the increase in LWCS, we used a line-by-line radiative transfer 1D column model (see the data availability statement for code and documentation). We prescribed in this radiative transfer model the Arctic temperature and moisture profiles from the different GCMs, averaged over regions that have at least 10% yearly maximum sea ice concentration at the start of the period of abrupt winter sea ice loss. Winter average profiles (DJF) corresponding to both before and after the period of abrupt sea ice change are used (Fig. S3 in the online supplemental material) to examine changes in the calculated LWCS during the years of winter sea ice loss. The radiative model was able to reproduce the change in winter average LWCS for each of the GCMs to within an error of about 10%. Increasing the specific humidity alone (without changing the atmospheric temperature profile) can account for a significant fraction (20%–30%) of the change in winter LWCS across the models. This is due to the lowering the effective level of downward thermal emission seen by the surface. The rest of the increase in LWCS can be explained by the atmospheric warming. Of course, the atmospheric temperature and specific moisture are coupled to each other, and their effects cannot be fully separated. However, we can conclude that both the moistening and warming of the lower atmosphere during the period of abrupt winter sea ice loss are key to driving the increases in LWCS at the surface.

Noting the extensive literature on the role of the lapse rate feedback in driving surface warming in the Arctic (Bintanja et al. 2011; Pithan and Mauritsen 2014; Feldl et al. 2020), we also choose to separate the LWCS PTC into a component driven by vertically uniform atmospheric warming and a component from changes in the lapse rate. To do this, we use the temperature profiles from before and after the period of abrupt sea ice loss (described in the paragraph above) to generate a “uniform warming” profile in which the vertically averaged warming of the troposphere between the start and end of the period is applied uniformly at all atmospheric levels below 300 hPa. We then run the LBL radiative transfer code with the two different temperature profiles (the actual end temperature profile and the uniform warming profile) and calculate the downwelling LWCS at the surface for both. We consider the difference in downwelling LWCS calculated between these two profiles to be the effect of the change in the

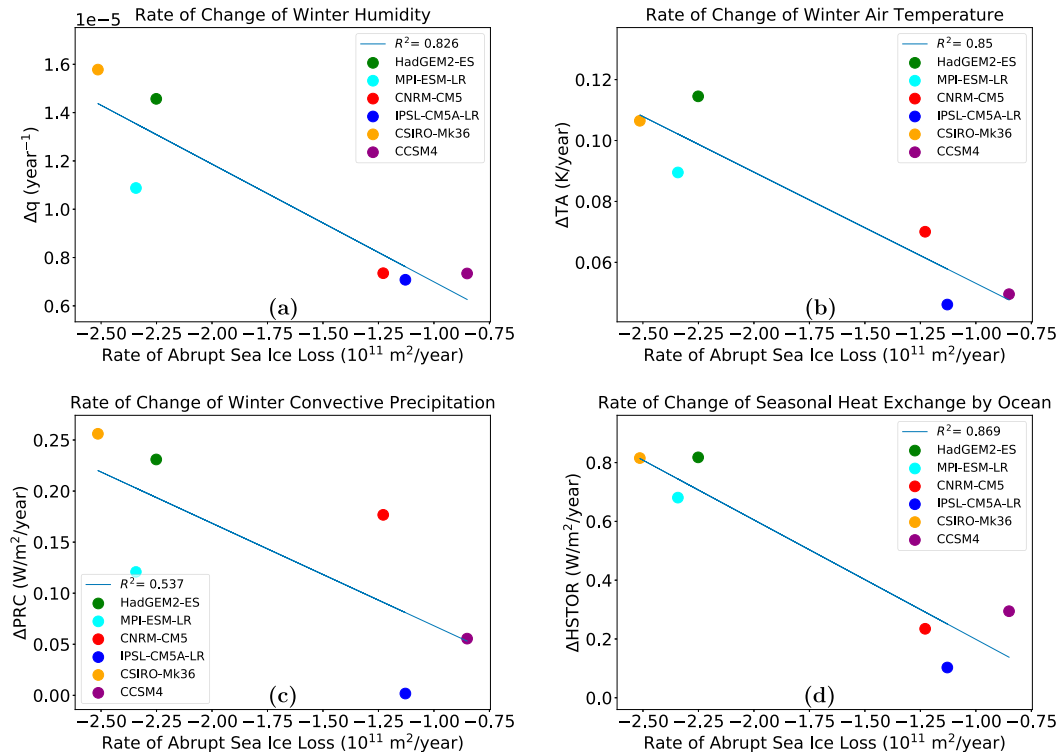


FIG. 4. Further insight into some of the feedbacks explored in this paper. First, there are processes that contribute to changes in LWCS radiation: (a) the rate of change of winter (a) specific humidity and (b) air temperature at 850 hPa during the period of abrupt sea ice loss. Then, there are processes that are related to cloud radiative effects: (c) the rate of change of convective precipitation, converted to watts per meter squared by using the latent heat of condensation. Third, there are processes that link spring and winter processes: (d) rate of change of seasonal heat exchange by the ocean, calculated as the difference between the (positive) average net radiative heat flux into in the spring (MAM) and summer (JJA) months and the (negative) average net heat flux into the ocean in autumn (SON) and winter (DJF).

lapse rate. We then convert the ΔLWCS due to lapse-rate changes into a PTC by dividing by $4\sigma T_s^3$. Although there is not a strong correlation between the lapse rate feedback PTC and the metric for abrupt sea ice loss (Fig. 2g), this analysis revealed that the lapse rate feedback accounted for between 0% and ~50% of the annual LWCS PTC across models. In the wintertime average, the lapse rate feedback accounted for between 15% and 45% of the winter component of LWCS PTC. Thus, we find that the lapse rate feedback is important for surface warming during the period of abrupt sea ice loss, although less dominant than it was found to be by Bintanja et al. (2011) and Pithan and Mauritsen (2014) in the case of twenty-first-century warming. This is likely because surface temperature inversions are weak or even nonexistent (both in the annual average and in the winter average) by the time winter sea ice starts to rapidly disappear.

With only six models and one ensemble each, the R^2 in Fig. 2 should not be overinterpreted. The linear regression analysis is still useful because it allows us to visually examine if there is a continuous range in the strength of this feedback and in the abruptness of the sea ice loss across models, explicitly testing our hypothesis. The statistically significant R^2 values in

Figs. 2a–c,e,f are very robust and did not drop below values corresponding to 95% significance level even when we used other metrics for quantifying the models' levels of abruptness of winter sea ice loss. Some of the metrics explored included the fraction of initial sea ice area lost in one period without any regrowth, and the absolute value of sea ice area lost in the year ranges used here.

Nonetheless, we find that an analysis that does not rely on a specific metric for quantifying the abruptness of winter sea ice loss is also useful. The six models can be visually divided into those with significant abrupt winter sea ice loss (CSIRO Mk3.6, MPI-ESM-LR, and HadGEM2-ES) and those with gradual winter sea ice loss (IPSL-CM5A-LR, CNRM-CM5, and CCSM4) based on the time series in Fig. 1a. In addition, our metric for quantifying the abruptness of winter sea ice loss separates the models into these exact same clusters (see the x -axis values in Fig. 2). We therefore choose to also present the PTCs as averages for the three models with abrupt sea ice loss and the three models with gradual sea ice loss. This analysis is shown as a bar plot in Fig. 3. We see that the main conclusions from Fig. 2 hold when considering the models in two discrete groups, and that nearly all yearly PTCs are larger for models

with abrupt winter sea ice loss (orange bars), consistent with their stronger feedback cycle. Additionally, the rightmost bars of Fig. 3 show the degree of annual Arctic amplification between the beginning and end of the simulation for both groups of models. We note that Boeke and Taylor (2018) found that a strong positive feedback cycle similar to the one invoked here led to enhanced Arctic amplification by year 2100. We find, though, that the models with a strong positive feedback during the period of abrupt winter sea ice loss are not necessarily those that have the most Arctic amplification over the entire extended RCP8.5 simulation until 2300. This does not necessarily contradict the findings of Boeke and Taylor (2018) because it is possible that the models with a strong feedback and large PTCs during the years of abrupt winter sea ice loss are not the same as those that have a strong feedback over the entire simulation.

As spring albedo decreases, one might expect that downwelling SW radiation at the surface (as opposed to absorbed SW by the surface) also decreases due to reduced multiple reflection between the surface and clouds, and due to increased SW clear-sky absorption by the atmosphere. Both of these effects counteract the warming by the surface albedo feedback. In particular, because we have seen that the models with more abrupt sea ice loss have more rapidly increasing atmospheric humidity (Fig. 4a), their additional absorption of SWCS by water vapor acts as a negative feedback. However, we see from Fig. 3 that the positive SAF PTC is much larger in magnitude than the CRE and SWCS PTCs combined. The near-zero CRE PTC for both groups of models is, in fact, due to cancellation between a small positive LW CRE component and a small negative SW CRE component, but the SW component combined with the negative SWCS PTC still does not outweigh the SAF PTC. We also see in Fig. S4 in the online supplemental material that, while downwelling SW and upwelling SW both decrease during the years of abrupt winter sea ice loss, the reduction of upwelling outweighs that of downwelling and thus leads to an increase of absorbed SW at the surface.

The reason that the surface albedo feedback is stronger in some models than others is not fully explored in this study, but we briefly offer some insight. First, we found that models with more abrupt winter sea ice area loss experienced a larger change in absolute surface albedo for a standardized loss of sea ice area (loss from 75% to 25% sea ice concentration; not shown). This highlights the fact that surface albedo depends on several other features besides sea ice area, such as the behavior of melt ponds, snow, and sea ice thickness. In particular, using the SIT output variable from CMIP5 revealed that models with more abrupt sea ice area loss also had faster rates of thinning; however, it should be noted that the SIT variable is an “effective” sea ice thickness (defined as the average thickness over the entire ocean portion, including the ice-free fraction). This means that the processes of sea ice thinning and area loss are not fully separated, and further investigation is required to understand how sea ice thinning affects the surface albedo feedback.

If changes in LWCS and absorbed SW radiation indeed drive the suppression of sea ice regrowth through their corresponding PTCs as we have shown, we would expect them to

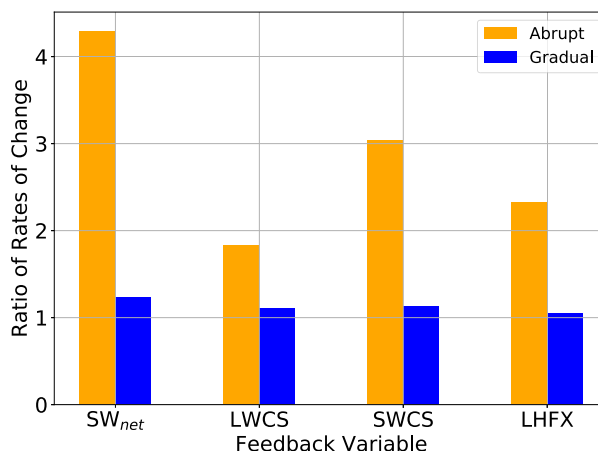


FIG. 5. Bars show the ratio of the rates of change of feedback variables during the period of abrupt winter sea ice loss to the rates of change during the entire simulation, as averages for the two groups of models. The variable SW_{net} represents absorbed shortwave radiation at the surface and does not correspond directly to a calculated PTC because it includes both changes in surface albedo and changes in downwelling SW radiation.

drive increases in the net radiation at the surface Q . However, the adjustment time scales of the surface temperature and therefore of the upwelling LW are shorter than the monthly data resolution. As a result, changes in the net surface flux in the Arctic average appear close to zero during the transition when examining the time series of Q (not shown). The positive PTCs for Q (although with very small magnitude for models with gradual sea ice loss) shown in Fig. 3 actually correspond to a decrease in Q over the period of abrupt sea ice loss because increasing surface temperature increases upwelling LW radiation as the system equilibrates back toward a balanced energy budget.

We see no obvious period of abrupt change in the time series of variables associated with positive feedbacks at the same time as the sea ice tipping point (although these variables are closely coupled to sea ice) except for in the case of absorbed SW radiation, in part due to the large “noise” present in these other variables. However, we can consider the average rate of change of key feedback variables during the period of abrupt sea ice loss compared to their rate of change over the entire simulation to further address this issue. Figure 5 shows the ratio of the rate of change of the given feedback variable poleward of 70°N and during the period of abrupt sea ice loss to the rate of change of the variable over the entire simulation. That all of the variables represented in Fig. 5 have a value well above 1 for models with abrupt sea ice loss (orange bars) demonstrates that they experience accelerated change in conjunction with the period of abrupt sea ice loss. The variables shown in this figure, LWCS, LHFx, and SW_{net} (which combines albedo and downward SW changes) have been found using the PTC analysis to be important components of the feedback cycle. In particular, increases in absorbed shortwave radiation are more than 4 times as fast during period of abrupt sea ice loss compared to the simulation as a whole. On the other hand, for models with

gradual winter sea ice loss (blue bars) the rates of change of the feedback variables shown are nearly the same during the period of winter sea ice loss and over the whole simulation. Thus, even though key variables such as LWCS do not qualitatively show a period of abrupt change upon inspection of their time series, we conclude from Fig. 5 that in models with a qualitative tipping point in winter sea ice area they do experience faster changes during the period of abrupt sea ice loss when compared with the entire simulation, whereas in models without a qualitative tipping point they do not.

For the feedback to get stronger from year to year without being broken by the seasonal cycle, the ocean needs to serve as the system's memory and couple the spring and winter mechanisms. The ocean can store the extra heat gained from having a lower surface albedo in spring and summer until the following winter when the warmed ocean then sets the conditions for greater latent heat fluxes and greater downwelling longwave radiation. This, in turn, can suppress sea ice growth and lead to lower albedo in spring (Boeke and Taylor 2018). That the ocean temperature anomalies imparted by reduced sea ice cover remain until the sea ice growing season is supported by previous studies (Blanchard-Wrigglesworth et al. 2011; Krikken and Hazeleger 2015). Figure 4d examines the seasonal ocean memory (following Boeke and Taylor 2018) by plotting the change in the difference between the net heat absorbed by the ocean in the spring and summer, and that released in the autumn and winter, versus the abruptness of winter sea ice loss. The tight correlation is consistent with ocean serving as the memory between seasons, and doing so more effectively in the models that have more abrupt sea ice loss. Thus, the seasonal heat exchange by the ocean allows the additional absorbed heat due to the reduced albedo in spring/summer to induce the suppression of winter sea ice growth the following year.

We now analyze the spatial distribution of the two key mechanisms in the proposed feedback cycle—the surface albedo feedback and clear-sky LW radiation—to demonstrate the local nature of the feedback. We wish to test our implicit assumption that the changes in Arctic-averaged variables such as LWCS are related to *local* changes in sea ice area, which in turn are related to *local* changes in absorbed shortwave. This is because the mechanism relies on the local coupling of the atmosphere and ocean, rather than on remote coupling (Boeke and Taylor 2018; D.-S. R. Park et al. 2015; H.-S. Park et al. 2015; Gong et al. 2017). We calculate the spatial correlation coefficient between the spring component of the SAF PTC and the winter component of the LWCS PTC. The color shading in Fig. 6 shows the spring SAF PTC at each grid point and the black contours represent the winter LWCS PTC. The spatial correlation coefficient of the two PTCs is shown in the upper left of each map. The strong correlations for all models, but in particular for models that experience abrupt sea ice loss, between the two PTCs that are separated temporally by the summer and autumn seasons again support the role of the ocean in transferring extra heat absorbed locally in the spring to the subsequent winter season. This highlights the

importance of the *local* nature of the positive feedback leading to abrupt winter sea ice loss.

4. Conclusions

In this study, we have proposed a year-to-year positive feedback cycle whose strength can explain the variability in the abruptness of winter Arctic sea ice loss simulated across CMIP5 global climate models in the extended RCP8.5 scenario. The mechanism involves wintertime LWCS increases due to a moister and warmer atmosphere, and a springtime surface albedo feedback due to reduced sea ice growth, linked by ocean seasonal heat storage that serves as a year-to-year memory. We quantify the strength of this positive feedback by examining the partial temperature contributions (Boeke and Taylor 2018) per unit time of the different surface heat fluxes that play a role in the feedback (LWCS, changes in absorbed SW due to reduced surface albedo, turbulent heat fluxes, etc.) during the period of abrupt sea ice loss. We then find that the feedback strength correlates with the abruptness of winter sea ice loss in these models. Thus, we conclude that this feedback mechanism plays a significant role in driving abrupt winter sea ice loss.

Bathiany et al. (2016) suggested that the freezing point of seawater exists as a natural threshold that can lead to abrupt disappearance of sea ice in the absence of any positive feedbacks. In the absence of feedbacks, the freezing threshold could, of course, lead to an abrupt winter sea ice loss if the Arctic Ocean temperature were uniform in space. We also agree with their conclusion that cloud feedbacks may not be the cause of the abrupt loss, although our findings indicate the importance of clear-sky LW radiation and moistening of the atmosphere. However, their mechanism cannot explain the spread in abruptness of sea ice loss between models, which we see here by plotting winter sea ice as a function of time (Fig. 1a) in addition to as a function of global surface temperature as done by Bathiany et al. (2016). The fact that sea ice area as a function of Arctic surface temperature (Fig. 7) is similar for all models suggests that the key difference across models is how quickly they move along the sea ice area versus surface temperature curve. The nonuniform ocean temperature in the Arctic means that the rate of ocean warming can influence the abruptness of winter sea ice loss. The freezing-point threshold does not explain the spread in ocean warming rates and therefore in abruptness, while the existence and strength of positive feedbacks can.

Abrupt changes often imply the existence of a bifurcation and thus hysteresis. However, in the case of winter sea ice loss the processes involved must be sufficiently nonlinear in order for the time series of sea ice area as the CO_2 is decreased to be different from that when the CO_2 is increased (i.e., hysteresis with respect to CO_2). There are some obvious nonlinearities involved in the proposed feedback, including the LW dependence on temperature via $\epsilon\sigma T^4$, the dependence of emissivity ϵ on moisture, and the ice-albedo feedback, which is known, of course, to be a strongly nonlinear process that produces hysteresis (e.g., Budyko 1969; Sellers 1969). A simpler model may be able to address whether the year-to-year positive feedback

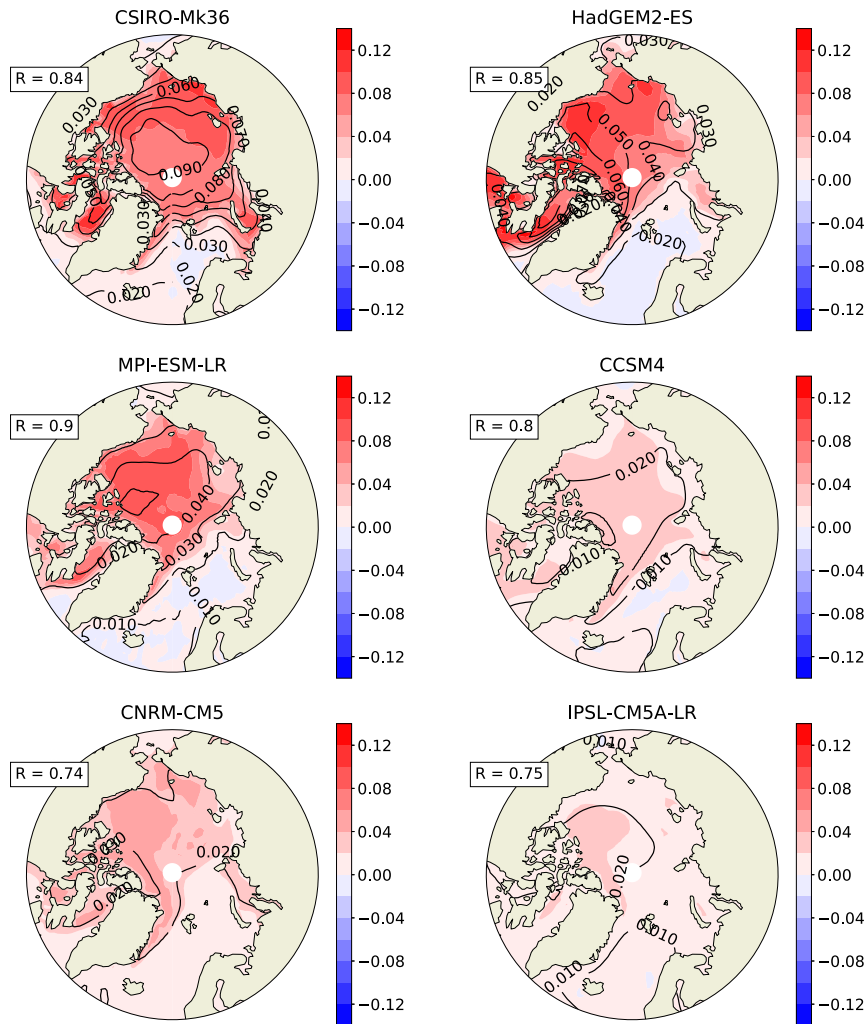


FIG. 6. Color shading shows the yearly *spring* component of the surface albedo feedback PTC at each grid point (K yr^{-1}), and black contours show the yearly *winter* component of the LWCS PTC at each grid point (K yr^{-1}). The R values show the calculated spatial correlation coefficient between these two seasonal PTCs for each model, revealing good correlation for all models but especially those with abrupt winter sea ice loss (CSIRO, HadGEM, and MPI).

proposed here is sufficiently nonlinear to produce such hysteresis.

We also note that we have not included a robust analysis of the role of remote heat and moisture transport mechanisms in driving intermodel spread of abrupt winter sea ice loss. Both atmospheric and oceanic poleward heat transport tend to decrease over global warming simulations due to weaker temperature gradients (Hwang et al. 2011; Kay et al. 2012; Pithan and Mauritsen 2014; Stuecker et al. 2018), with decreasing atmospheric sensible heat flux dominating increasing latent heat flux. These fluxes are therefore unlikely to be part of a positive feedback mechanism, although a decreased heat transport could be considered a negative feedback that competes with the positive feedback analyzed here. As such, differences across models in the weakening of poleward heat

transport could contribute to differences in abrupt winter sea ice loss in ways we have not yet explored.

The predictability of Arctic sea ice area at present has been analyzed using lag correlations of sea ice anomalies in other work (Blanchard-Wrigglesworth et al. 2011; Kriken and Hazeleger 2015). Those studies found that the signal of sea ice area anomalies decays first according to a red-noise distribution, but then can potentially reemerge at a lag time of 2–5 months. The positive feedback proposed here may affect predictability in two ways. On the one hand, the time of transition to an ice-free winter is difficult to predict as it may involve the amplification by the positive feedback of any small fluctuation in key state variables. On the other hand, once a transition starts, the positive feedback is likely to lead to a complete ice-free winter state, reducing uncertainty at that point. Additionally, future studies could use a long control run to

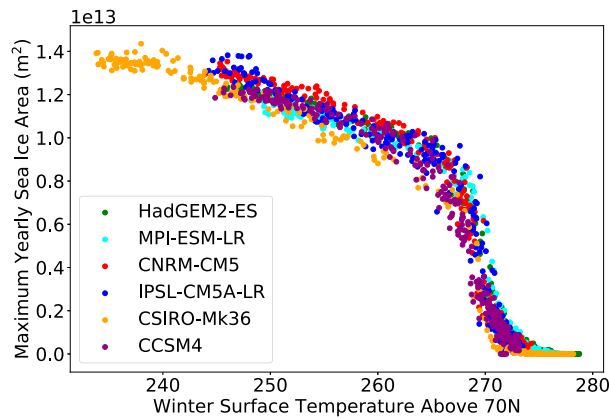


FIG. 7. Yearly maximum sea ice area plotted against average surface temperature poleward of 70°N for all six models. The relationship between Arctic winter sea ice area and surface temperature appears to be similar for all models.

examine the strength of the mentioned feedbacks in shorter or more localized abrupt sea ice loss events, to see if the same mechanisms as those proposed here are also the driving sea ice loss at smaller spatial and temporal scales. If the effect of local feedbacks on sea ice is robust at smaller scales, this relationship could be used to predict the likelihood of a future large-scale tipping-point event. Such a change in our predictive capabilities would significantly affect the way we plan for a perennially ice-free Arctic in the future.

Acknowledgments. We thank three anonymous reviewers for their constructive and helpful comments. This work was supported by the National Science Foundation Climate Dynamics Program for NSF/NERC collaborations, Grant AGS-1924538. Author Tziperman thanks the Weizmann Institute for its hospitality during parts of this work.

Data availability statement. CMIP5 output data for all models except CCSM4 are hosted by the U.S. Department of Energy Lawrence Livermore National Laboratory (<https://esgf-node.llnl.gov/search/cmip5/>). Output data for model CCSM4 are hosted by NCAR (<https://www.earthsystemgrid.org/search.html>). The line-by-line radiative transfer model was built by author Hankel as part of required coursework at Harvard University and is available online (https://osf.io/qkbje/?view_only=23d357413bce43c8a6de974ae971a948). It uses molecular absorption data from the HITRAN line-by-line database (accessible at <https://hitran.org/>) and atmospheric constituent profiles from Anderson et al. (1986).

REFERENCES

- Abbot, D. S., and E. Tziperman, 2008a: A high-latitude convective cloud feedback and equable climates. *Quart. J. Roy. Meteor. Soc.*, **134**, 165–185, <https://doi.org/10.1002/qj.211>.
- , and —, 2008b: Sea ice, high-latitude convection, and equable climates. *Geophys. Res. Lett.*, **35**, L03702, <https://doi.org/10.1029/2007GL032286>.
- , and —, 2009: Controls on the activation and strength of a high-latitude convective-cloud feedback. *J. Atmos. Sci.*, **66**, 519–529, <https://doi.org/10.1175/2008JAS2840.1>.
- , C. Walker, and E. Tziperman, 2009: Can a convective cloud feedback help to eliminate winter sea ice at high CO₂ concentrations? *J. Climate*, **22**, 5719–5731, <https://doi.org/10.1175/2009JCLI2854.1>.
- , M. Silber, and R. T. Pierrehumbert, 2011: Bifurcations leading to summer Arctic sea ice loss. *J. Geophys. Res.*, **116**, D19120, <https://doi.org/10.1029/2011JD015653>.
- Anderson, G. P., S. A. Clough, F. Kneizys, J. H. Chetwynd, and E. P. Shettle, 1986: AFGL atmospheric constituent profiles (0.120 km). Air Force Geophysics Laboratory (Hanscom Air Force Base) Tech. Rep., 46 pp.
- Armour, K., I. Eisenman, E. Blanchard-Wrigglesworth, K. McCusker, and C. Bitz, 2011: The reversibility of sea ice loss in a state-of-the-art climate model. *Geophys. Res. Lett.*, **38**, L16705, <https://doi.org/10.1029/2011GL048739>.
- Arnold, N., M. Branson, M. A. Burt, D. S. Abbot, Z. Kuang, D. A. Randall, and E. Tziperman, 2014: Effects of explicit atmospheric convection at high CO₂. *Proc. Natl. Acad. Sci. USA*, **111**, 10 943–10 948, <https://doi.org/10.1073/pnas.1407175111>.
- Bathiany, S., D. Notz, T. Mauritsen, G. Raedel, and V. Brovkin, 2016: On the potential for abrupt Arctic winter sea ice loss. *J. Climate*, **29**, 2703–2719, <https://doi.org/10.1175/JCLI-D-15-0466.1>.
- Bintanja, R., R. Graversen, and W. Hazeleger, 2011: Arctic winter warming amplified by the thermal inversion and consequent low infrared cooling to space. *Nat. Geosci.*, **4**, 758–761, <https://doi.org/10.1038/ngeo1285>.
- Blanchard-Wrigglesworth, E., K. C. Armour, C. M. Bitz, and E. DeWeaver, 2011: Persistence and inherent predictability of Arctic sea ice in a GCM ensemble and observations. *J. Climate*, **24**, 231–250, <https://doi.org/10.1175/2010JCLI3775.1>.
- Block, K., and T. Mauritsen, 2013: Forcing and feedback in the MPI-ESM-LR coupled model under abruptly quadrupled CO₂. *J. Adv. Model. Earth Syst.*, **5**, 676–691, <https://doi.org/10.1002/jame.20041>.
- Boeke, R. C., and P. C. Taylor, 2018: Seasonal energy exchange in sea ice retreat regions contributes to differences in projected Arctic warming. *Nat. Commun.*, **9**, 5017, <https://doi.org/10.1038/s41467-018-07061-9>.
- Budyko, M. I., 1969: The effect of solar radiation variations on the climate of the earth. *Tellus*, **21**, 611–619, <https://doi.org/10.3402/tellusa.v21i5.10109>.
- Burt, M. A., D. A. Randall, and M. D. Branson, 2016: Dark warming. *J. Climate*, **29**, 705–719, <https://doi.org/10.1175/JCLI-D-15-0147.1>.
- Drijfhout, S., and Coauthors, 2015: Catalogue of abrupt shifts in Intergovernmental Panel on Climate Change climate models. *Proc. Natl. Acad. Sci. USA*, **112**, E5777–E5786, <https://doi.org/10.1073/pnas.1511451112>.
- Eisenman, I., 2007: Arctic catastrophes in an idealized sea ice model. 2006 Program of Studies: Ice, Woods Hole Oceanographic Institution Geophysical Fluid Dynamics Program Tech. Rep. 2007-02, 133–161, <http://www.gps.caltech.edu/~ian/publications/Eisenman-2007.pdf>.
- , 2012: Factors controlling the bifurcation structure of sea ice retreat. *J. Geophys. Res.*, **117**, D01111, <https://doi.org/10.1029/2011JD016164>.
- , and J. S. Wettlaufer, 2009: Nonlinear threshold behavior during the loss of Arctic sea ice. *Proc. Natl. Acad. Sci. USA*, **106**, 28–32, <https://doi.org/10.1073/pnas.0806887106>.
- Feldl, N., S. Po-Chedley, H. K. Singh, S. Hay, and P. J. Kushner, 2020: Sea ice and atmospheric circulation shape the high-latitude lapse rate feedback. *npj Climate Atmos. Sci.*, **3**, 41, <https://doi.org/10.1038/s41612-020-00146-7>.

- Gong, T., S. Feldstein, and S. Lee, 2017: The role of downward infrared radiation in the recent Arctic winter warming trend. *J. Climate*, **30**, 4937–4949, <https://doi.org/10.1175/JCLI-D-16-0180.1>.
- Goosse, H., and Coauthors, 2018: Quantifying climate feedbacks in polar regions. *Nat. Commun.*, **9**, 1919, <https://doi.org/10.1038/s41467-018-04173-0>.
- Hezel, P., T. Fichefet, and F. Massonnet, 2014: Modeled Arctic sea ice evolution through 2300 in CMIP5 extended RCPs. *Cryosphere*, **8**, 1195–1204, <https://doi.org/10.5194/tc-8-1195-2014>.
- Holland, M. M., C. M. Bitz, and B. Tremblay, 2006: Future abrupt reductions in the summer Arctic sea ice. *Geophys. Res. Lett.*, **33**, L23503, <https://doi.org/10.1029/2006GL028024>.
- Hwang, Y.-T., D. M. Frierson, and J. E. Kay, 2011: Coupling between Arctic feedbacks and changes in poleward energy transport. *Geophys. Res. Lett.*, **38**, L17704, <https://doi.org/10.1029/2011GL048546>.
- Kay, J. E., M. M. Holland, C. M. Bitz, E. Blanchard-Wrigglesworth, A. Gettelman, A. Conley, and D. Bailey, 2012: The influence of local feedbacks and northward heat transport on the equilibrium Arctic climate response to increased greenhouse gas forcing. *J. Climate*, **25**, 5433–5450, <https://doi.org/10.1175/JCLI-D-11-00622.1>.
- Krikken, F., and W. Hazeleger, 2015: Arctic energy budget in relation to sea ice variability on monthly-to-annual time scales. *J. Climate*, **28**, 6335–6350, <https://doi.org/10.1175/JCLI-D-15-0002.1>.
- Leibowicz, B. D., D. S. Abbot, K. Emanuel, and E. Tziperman, 2012: Correlation between present-day model simulation of Arctic cloud radiative forcing and sea ice consistent with positive winter convective cloud feedback. *J. Adv. Model. Earth Syst.*, **4**, M07002, <https://doi.org/10.1029/2012MS000153>.
- Lu, J., and M. Cai, 2009a: A new framework for isolating individual feedback processes in coupled general circulation climate models. Part I: Formulation. *Climate Dyn.*, **32**, 873–885, <https://doi.org/10.1007/s00382-008-0425-3>.
- , and —, 2009b: Seasonality of polar surface warming amplification in climate simulations. *Geophys. Res. Lett.*, **36**, L16704, <https://doi.org/10.1029/2009GL040133>.
- Notz, D., 2009: The future of ice sheets and sea ice: Between reversible retreat and unstoppable loss. *Proc. Natl. Acad. Sci. USA*, **106**, 20 590–20 595, <https://doi.org/10.1073/pnas.0902356106>.
- Park, D.-S. R., S. Lee, and S. B. Feldstein, 2015: Attribution of the recent winter sea ice decline over the Atlantic sector of the Arctic Ocean. *J. Climate*, **28**, 4027–4033, <https://doi.org/10.1175/JCLI-D-15-0042.1>.
- Park, H.-S., S. Lee, S.-W. Son, S. B. Feldstein, and Y. Kosaka, 2015: The impact of poleward moisture and sensible heat flux on Arctic winter sea ice variability. *J. Climate*, **28**, 5030–5040, <https://doi.org/10.1175/JCLI-D-15-0074.1>.
- Pithan, F., and T. Mauritsen, 2014: Arctic amplification dominated by temperature feedbacks in contemporary climate models. *Nat. Geosci.*, **7**, 181–184, <https://doi.org/10.1038/ngeo2071>.
- Ridley, J., J. Lowe, and H. Hewitt, 2012: How reversible is sea ice loss? *Cryosphere*, **6**, 193–198, <https://doi.org/10.5194/tc-6-193-2012>.
- Screen, J. A., and I. Simmonds, 2010: Increasing fall–winter energy loss from the Arctic Ocean and its role in Arctic temperature amplification. *Geophys. Res. Lett.*, **37**, L16707, <https://doi.org/10.1029/2010GL044136>.
- Sellers, W. D., 1969: A global climate model based on the energy balance of the Earth–atmosphere system. *J. Appl. Meteor.*, **8**, 392–400, [https://doi.org/10.1175/1520-0450\(1969\)008<0392:AGCMBO>2.0.CO;2](https://doi.org/10.1175/1520-0450(1969)008<0392:AGCMBO>2.0.CO;2).
- Smith, D. M., N. J. Dunstone, A. A. Scaife, E. K. Fiedler, D. Copsey, and S. C. Hardiman, 2017: Atmospheric response to Arctic and Antarctic sea ice: The importance of ocean–atmosphere coupling and the background state. *J. Climate*, **30**, 4547–4565, <https://doi.org/10.1175/JCLI-D-16-0564.1>.
- Soden, B. J., I. M. Held, R. Colman, K. M. Shell, J. T. Kiehl, and C. A. Shields, 2008: Quantifying climate feedbacks using radiative kernels. *J. Climate*, **21**, 3504–3520, <https://doi.org/10.1175/2007JCLI2110.1>.
- Stuecker, M. F., and Coauthors, 2018: Polar amplification dominated by local forcing and feedbacks. *Nat. Climate Change*, **8**, 1076–1081, <https://doi.org/10.1038/s41558-018-0339-y>.
- Taylor, K. E., R. J. Stouffer, and G. A. Meehl, 2012: An overview of CMIP5 and the experiment design. *Bull. Amer. Meteor. Soc.*, **93**, 485–498, <https://doi.org/10.1175/BAMS-D-11-00094.1>.
- Taylor, P. C., M. Cai, A. Hu, J. Meehl, W. Washington, and G. J. Zhang, 2013: A decomposition of feedback contributions to polar warming amplification. *J. Climate*, **26**, 7023–7043, <https://doi.org/10.1175/JCLI-D-12-00696.1>.
- , B. M. Hegyi, R. C. Boeke, and L. N. Boisvert, 2018: On the increasing importance of air–sea exchanges in a thawing Arctic: A review. *Atmosphere*, **9**, 41, <https://doi.org/10.3390/atmos9020041>.
- Wagner, T. J., and I. Eisenman, 2015: How climate model complexity influences sea ice stability. *J. Climate*, **28**, 3998–4014, <https://doi.org/10.1175/JCLI-D-14-00654.1>.
- Winton, M., 2006: Does the Arctic sea ice have a tipping point? *Geophys. Res. Lett.*, **33**, L23504, <https://doi.org/10.1029/2006GL028017>.